Available online at www.sciencedirect.com
ScienceDirect
Coordination Chemistry Reviews 251 (2007) 2688–2701
COORDINATION CHEMISTRY REVIEWS
www.elsevier.com/locate/ccr

Review

Fabrication and functions of surface nanomaterials based on multilayered or nanoarrayed assembly of metal complexes

Masa-aki Haga *, Katsuaki Kobayashi, Keiichi Terada

Department of Applied Chemistry, Faculty of Science and Engineering, Chuo University, 1-13-27 Kasuga, Bunkyo, Tokyo 112-8551, Japan

Received 20 February 2007; accepted 30 March 2007
Available online 5 April 2007

Contents

Abstract

The bottom–up approach to functional nanoscale architectures from molecular components at the surface is the fundamental subject of nanomaterial science. This review addresses the recent advances in coordination multilayered architectures based on metal complexes, and discusses the potential applications in photo- and electrochemical devices. Following self-assembly of an anchor monolayer on solid surface, layer-by-layer growth of the molecular units proceeded with the assistance of metal coordination, resulting in multilayer structures. Particular emphasis is placed on the use of multipod anchoring groups immobilized on surface in order to fix the molecular orientation in a rigid and well-ordered manner. The fixed arrangement of molecular units on surface affords a uniform response to external stimuli and a predetermined distance for electron transfer on the electrode surface, which provides novel molecular electronic devices. An interconnection between two terminals by assembling molecular components is an emerging research target at the nanometer scale. New method for the DNA capture is developed by use of a DNA intercalator metal complex immobilized on surface. Utilizing the DNA capturing ability of the immobilized complex, DNA-templated nanowiring on a Au/SiO_2 patterned surface is achieved by selective anchoring of thiol/phosphonate groups, followed by the layering of DNA intercalator on the surface.

Keywords: Metal complexes; Surface coordination; Multilayer; Nanomaterials; Nanowire; DNAwire; Self-assembly; Redox-active complex

1. Introduction

The bottom–up assembly of functional nanoscale architecture from molecular components at the surface has attracted much interest in the advancement of nano-technology [1–6]. Particularly, the chemistry of surface modification by self-assembled monolayers (SAM) and layer-by-layer (LbL) growth

* Corresponding author. Tel.: +81 3 3817 1908; fax: +81 3 3817 1895.
E-mail address: mhaga@chem.chuo-u.ac.jp (M.-a. Haga).

0010-8545/$ – see front matter © 2007 Elsevier B.V. All rights reserved.
doi:10.1016/j.ccr.2007.03.022

of multilayers is highly promising to construct two-dimensional (2D) and three-dimensional (3D) chemical systems on surfaces [7,8].

Alkanethiol self-assembly onto gold is the most widely studied example to modulate interfacial properties such as wettability, adhesion, tribology, and biocompatibility [9,10]; however, the utility of gold-thiol SAM chemistry is limited because of low integration of functional molecular units and the lack of a general fabrication route to more complex, multilayer structures. On the other hand, the sequential LbL assembly of multiple layers has a much broader benefit from the abundance of the combination of functional molecular components in the vertical direction, which determines the multilayer properties. Several rational fabrication methods for multilayer structures on surfaces have been developed, classified by the type of interaction between the layers; i.e., electrostatic interaction, hydrogen bonding interaction, and coordination bond [7,11]. In particular, LbL multilayer formation by metal ion coordination using bifunctional ligand building blocks has been studied in a variety of systems, including alkylmercaptocarboxylate/Cu(II) [12], Ru_3-cluster/4,4′-bipyridine [13], metal–metal bonded Ru_2-dimer/bipyrdine [14], azobis(terpyridine)/Fe(II) or Co(II) [15], surface-active *N*-[(3-trimethoxysilyl)propyl] ethylenediaminetriacetate-Ru complex/pyrazine [16], and $Ni^{2+}/Pt(CN)_4{}^{2-}$/4,4′-bipyridine [17]. Incorporation of redox-active molecular units within multilayer films makes it possible to create an appropriate potential gradient for vectorial electron transfer, and also an electrochemical response site [18]. As a functional electron transfer multicomponent system, a natural photosynthetic membrane is a good example, which consists of pigment–protein complexes, reaction center proteins, and catalytic sites. Each component has its own task, such as light harvesting, charge-separation, and conversion of the electron transfer process into electrochemical potential energy, and redox catalytic reaction etc., and is organized as one functional system; therefore, the construction of an artificial photosynthetic system is an important goal for functional multilayer systems [19–21].

Another aspect of nanoscale molecular systems on surfaces is the enormous promise and enormous challenge against scaling limits of transistors in conventional silicon-based microelectronic devices, which has shrunk to the nanometer (less than 100 nm) size regime [1,22]. Molecular-scale devices are an emerging technology representing the ultimate in device scaling at molecular lengths of ∼1 nm. A great challenge is to assemble the molecules into pre-patterned surfaces fabricated by photolithographic methods and to interconnect the terminals. The assembly of discrete molecular units affords two-dimensional and three-dimensional topological structures through various combinations of molecular units and diverse functionality through the structure/function relationship in molecular devices [4,23–25].

In this review, we focus mainly on surface molecular-based materials, which have a multilayered structure or have the potential for interconnecting two prepatterned inorganic surfaces (Scheme 1). Our objectives are to present our perspective of a surface coordination space and to summarize current efforts toward the nanofabrication of molecular devices from the viewpoint of metal coordination chemistry. Several nice review articles can be found in the related fields [10,11,26,27].

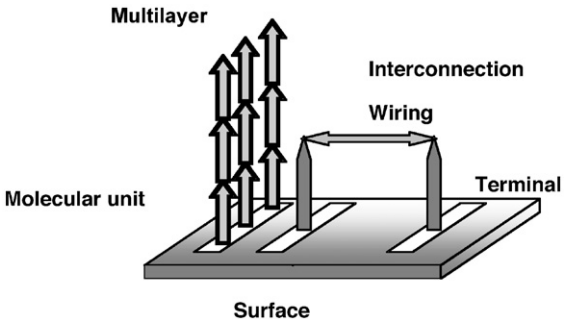

Scheme 1. Schematic drawing for multilayering and interconnection between two terminals.

2. Multilayered assembly built from molecular units on a surface

Self-assembled monolayers (SAMs) form as a result of spontaneous adsorption and organization of adsorbate molecules on a solid surface upon exposure to dilute solution. Since Allara and co-workers [9,28,29] found that a thiol group was attached on the gold surface, an element of functionality was added to SAMs, which lead to functional SAMs suitable for diverse applications such as electrode modification, biosensors, photoelectrochemical devices, and so on. Both head group and functional units in the adsorbate molecule are designed to introduce suitable functionality, allowing surface derivatization on the solid substrate such as Au or indium–tin oxide (ITO). Many metal complexes such as $Ru(bpy)_3$ [30], ferrocene [31], and porphyrin [32–34] can be self-assembled by thiol or disulfide anchor groups on an Au or ITO electrode, in which not only the basic electron transfer kinetics but also photocurrent generation or sensing properties have been explored. In addition to a thiol group self-assembled on the Au surface, other organic groups such as carboxylate, phosphonate, and isocyanide [35] are also recognized to act as surface-immobilized groups. In these organic anchoring groups, differential reactivity towards Au, Pt, and metal oxide, which is often called orthogonal self-assembly, has been reported; i.e., thiol and disulfide groups are preferentially bound to a gold substrate, [36] whereas isocyanide and pyridine groups are bound to a platinum surface, and phosphonate and silanol groups to indium tin oxide and metal oxide surfaces, respectively [37]. This surface selective modification is named by Wrighton as the “orthogonal self-assembly method” [38]. Both thiolate and phosphonate monolayer films are stable in aqueous solution over the pH range 1–9 [39,40]. Although thiol-gold self-assembled chemistry has been extensively studied, phosphonate-metal oxide self-assembled chemistry is still not mature. As for phosphonate-metal oxide self-assembled chemistry, the growth mechanism of long alkyl chain phosphonic acid on mica or sapphire has been investigated by Schwartz and co-workers [41,42]. They

reported that a continuous 2D phase of disordered molecules is formed initially and later evolves via thicker, more ordered film via the gradual growth of higher structures at room temperature. At lower temperatures, the monolayer forms by nucleation and the growth of ligands in which molecules are close-packed and vertically oriented. Furthermore, direct attachment of organophosphonic acid to the SiO_2/Si surface has been accomplished by the method of tethering by aggregation and growth at 140 °C, referred to as the "T-BAG" method for short [43]. This "T-BAG" method was reported to give close-packed alkyl chains in octadecylphosphonate SAM on the SiO_2/Si surface. The "T-BAG" SAM of phosphonic acid can be removed from the SiO_2/Si surface by sonication in 0.5 M K_2CO_3 in 2:1 ethanol/water typically for 20 min, followed by extensive rinsing with water. Further, copious rinsing of Si samples with 5% dry triethylamine in THF also removes most SAM. The "T-BAG" method can be applied for the surface immobilization of phosphonic acid on other metal oxide surfaces such as ITO and TiO_2.

For the immobilization of phosphonate groups on ITO, glass, or SiO_2, priming was sometimes used. For example, glass and SiO_2 substrates were pretreated with aminopropylsilane and then phosphorylation with $POCl_3$ and collidine, followed by zirconation by aqueous $ZrOCl_2$ [44]. In the case of the TiO_2 substrate, exposure to $Zr(OBu^t)_4$ vapor with a hydroxylated TiO_2 surface enhanced the surface binding of organic phosphonic acid [45].

However, SAMs on surfaces have low absorptivity density even in a densely packed state, as collecting photons in photoelectrochemical devices and only a simple chemical event can be performed. On the other hand, in multilayer films, the chemical function of each layer can be additively combined to work as a one system with complicated functions. In order to fabricate multilayer film on the surface, electrostatic interaction between anionic and cationic polyelectrolytes is commonly used as an alternating layer-by-layer method. In the case of polymer electrolytes, the boundary between the two layers is not well-defined and polymer components are sometimes entangled [8]. Alternatively, a coordination bond between metal ions and anchored ligand is available for building up layered or extended structures on the surface.

2.1. Multiple surface attachment of self-assembled monolayer on solid surface

In order to respond to external stimuli, the regular arrangement of functional units is a prerequisite for a well-defined and uniform response of functional SAMs. Functional units such as metal complexes tend to disturb the lateral interactions responsible for SAM alkyl chain ordering because of their bulkiness, polarity etc. (Scheme 2). If molecular packing is low, the molecular orientation becomes disordered since simple alkyl chains are flexible; however, with mechanical motion of a "molecular arm" for certain biomedical applications such as DNA microarrays on the surface, sufficient spatial freedom around each SAM molecule is required (Scheme 3). Once a low-density SAM has been created, reversible conformational changes by

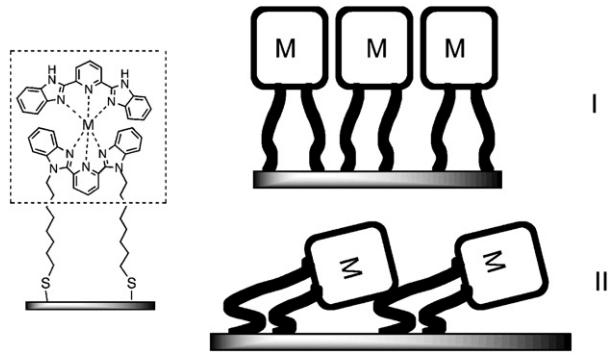

Scheme 2. Two different orientations of mononuclear Ru complex with simple alkylthiol groups on a gold surface: (I) well-ordered orientation, (II) disordered orientation.

external electrical potential [46,47] or high single nucleotide polymorphism (SNP) discrimination efficiency [48] can been demonstrated.

In order to control molecular spacing, a precursor SAM molecule with a bulky head group or cone-shaped dendron with multiple anchor sites has been used. To ensure the dynamic response to external stimuli, molecules with multiple attachment points are desirable to keep the molecular orientation rigid on the surface; examples are shown in Scheme 4.

The rigid tripod –COOH, $–P(O)(OH)_2$ or –SH surface binding groups having a tetrahedral core such as tetraphenylmethane or 1,3,5,7-tetraphenyladamantane provides a stable, three-point attachment to the solid surface [11,21,49–53]. Recently, four or more anchoring groups have also been reported [11,48]. These types of molecules with multiple anchoring ligands were bound strongly to the solid substrate, and the molecular orientation was fixed on surfaces. For example, in the photoelectrochemical multicomponent system, consisting of an electron sensitizer, electron donor and acceptors, the molecular arrangement at the surface plays an important role in the interfacial electron transfer reaction [20,54,55]. Further, [2]rotaxane with a tripodal phosphonate anchor group on a TiO_2 nanoparticle surface has been reported, in which a crown ether is threaded into a viologen-based axle [51,56]. In this rotaxane system, the shuttle movement of crown ether was controlled by the oxidation state of the viologen moiety.

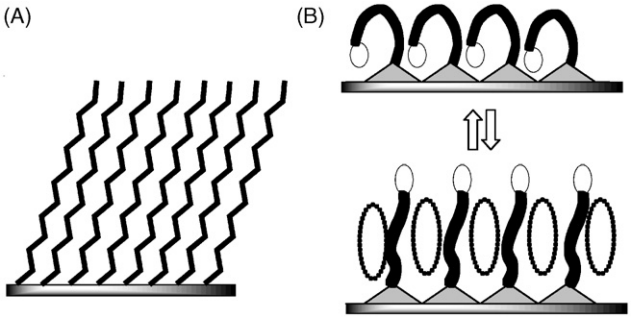

Scheme 3. Dense molecular packing (A) and loose molecular packing in SAM for reversible dynamic changes by external stimulus (B).

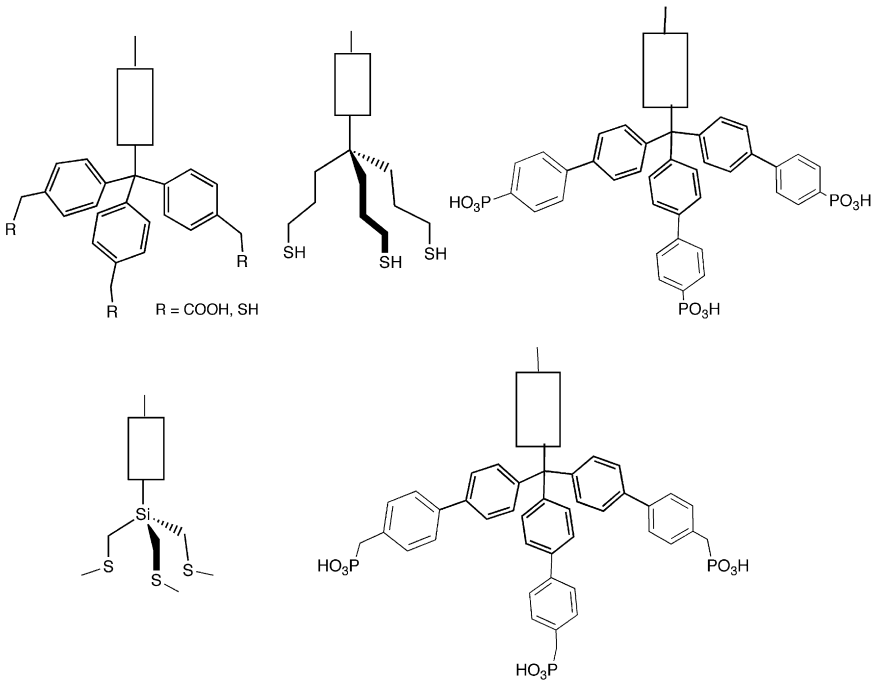

Scheme 4. Partial structures of multipod anchoring groups.

Recently, we have synthesized novel bi- and tetrapod anchoring ligands based on 2,6-bis(benzimidazol-2-yl)pyridine having two or four phosphonate or thiol groups (LP, XP, and LT, respectively) and their redox-active Ru/Os complexes (see Scheme 5) [18,57–59]. In particular, ligand XP has two mesityl groups with two auxiliary methylenephosphonic acids, which are oriented perpendicular to the 2-benzimidazolyl plane because of restricted rotation around C(mesityl))-C(methylene) and C(methylene)-*N*(benzimidazoly) bonds.

This molecular orientation was confirmed by the X-ray crystal structure of ethyl-protected $[Ru(Et\text{-}XP)(tpy)]^{2+}$, in which two planes of mesityl and 2-benzimidazolyl rings are perpendicularly oriented. By considering both the X-ray structure and molecular modeling, the four legs of phosphonate are directed to the metal oxide surface such as tin-doped indium oxide (ITO) or silicon oxide after deprotection of ethyl groups on Et-XP shown in Scheme 6. The height profiles of the atomic force microscope (AFM) for mononuclear and dinuclear complexes, $[Ru(XP)_2]$ and $[Ru_2(XP)_2(tpy\text{-}ph\text{-}tpy)]$, on a flat ITO substrate exhibit regular heights of 1.7 ± 0.1 and 3.8 ± 0.2 nm, respectively, which are consistent with those predicted from molecular modeling for the vertical orientation of molecules from the normal surface. A typical AFM image of dinuclear $[Ru_2(XP)_2(tpy\text{-}ph\text{-}tpy)]$ complexes on the flat ITO substrate is shown in Fig. 1. The packing density of the complex on ITO substrate was controlled by the concentration of the metal complex in solution. At a low concentration of the metal complex, scattered dots with an average height of -3.8 nm were observed, whereas at higher concentration, the whole surface was covered by closely packed monolayers. By using a tetrapod phosphonate anchor XP ligand, XP complexes can be directly bound to the ITO surface without any pretreatment of the surface.

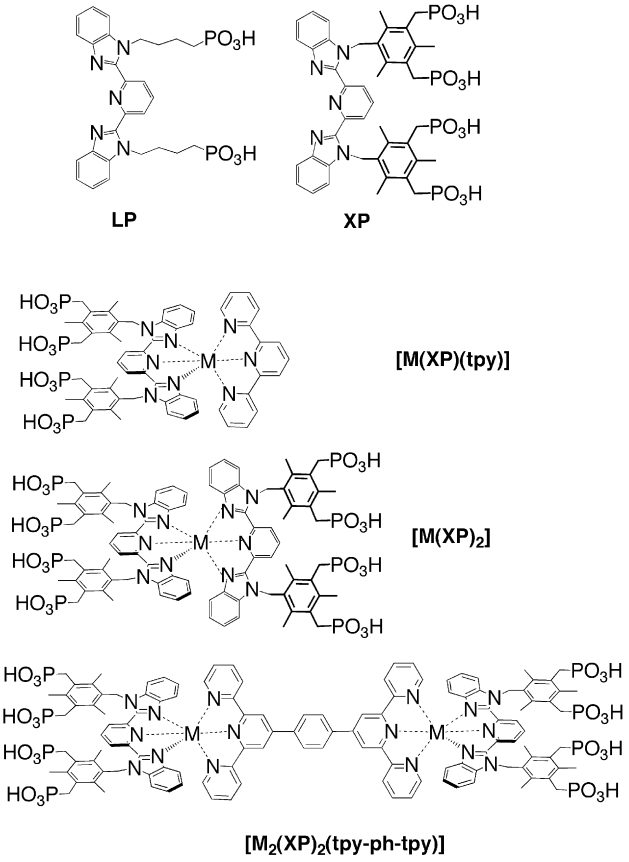

Scheme 5. Structures and abbreviations of anchoring ligands and metal complexes.

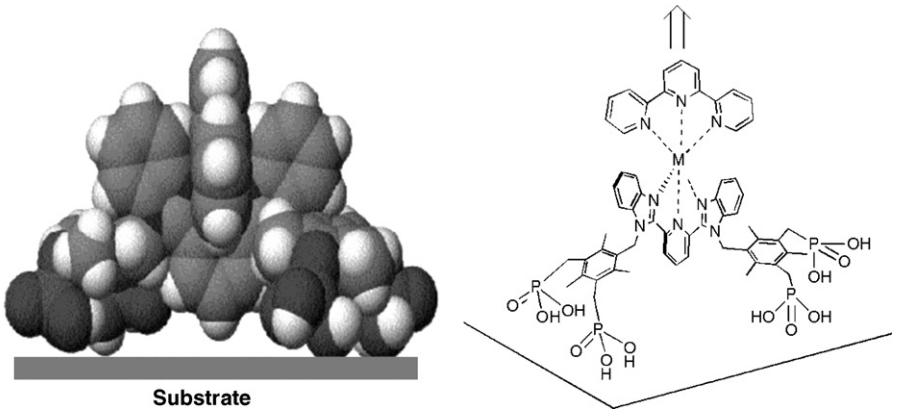

Scheme 6. Proposed molecular orientation of [M(XP)(tpy)] (Ref. [59]. ©Springer).

2.2. Fabrication of multilayered nanomaterials based on metal coordination

The "bottom–up" approach for multilayer construction using sequential LbL self-assembly provides the integration of molecular units into solid surfaces in a controlled manner at nanometer sizes. Several methods, which can be distinguished by the type of interaction between layers, have proven feasible. Electrostatic assembly, based on the sequential adsorption of polyanions and polycations, is a simple, but also powerful approach, which relies on electrostatic interaction between oppositely charged layers [8,60,61]. This methodology can be readily generalized to extend to a variety of polyelectrolyte materials such as polymers, nanoparticles, clay-like nanosheets, and even biomaterials (enzymes and proteins); however, this assembled method is known to present with irregular morphology, resulting in entanglement between layers. Hydrogen-bonding interactions [62,63], covalent assembly [64,65], and host–guest interactions [66,67] have also been developed for the construction of multilayer films. In one LbL method, multilayer formation by successive metal coordination on surfaces deserves attention, which is relevant to the "complexes-as-ligands" and/or "complexes-as-metals" strategy in solution for the synthesis of polynuclear or dendritic metal complexes [68]. In this method, primer SAM on the surface can act as a ligand to bind another metal ion, to which a ditopic linker is coordinated. The resulting second layer becomes the next bridging linker. By continuing this process, each layer is grown on the surface in a self-limiting manner to give well-defined nanometer-sized multilayers. From this "bottom–up" synthesis on a solid surface, multilayered architecture consisting of multicomponents can easily be fabricated by changing metal ions, ditopic molecular units, or organic linkers, as shown in Scheme 7. The selection of surfaces, anchored groups, functional molecular units and ditopic linker determines the functionality of multilayers. Alkylsilanol, thiol, and disulfide are generally used as an anchored group to a solid surface such as quartz or Au (see Section 2.1), whereas bipyridine, terpyridine, or isocyanide are applied for metal coordination groups. The reported examples of layer-by-layer inorganic supramolecular structures are shown in Scheme 8. For example, Nishihara and co-workers synthesized polymetallic complexes **2** on Au by alternate deposition of a Fe(II) complex unit with dinucleating azobenzene-bridged bis(terpyridine) ligand (tpy-AB-tpy) [15]. Similarly, Abruna et

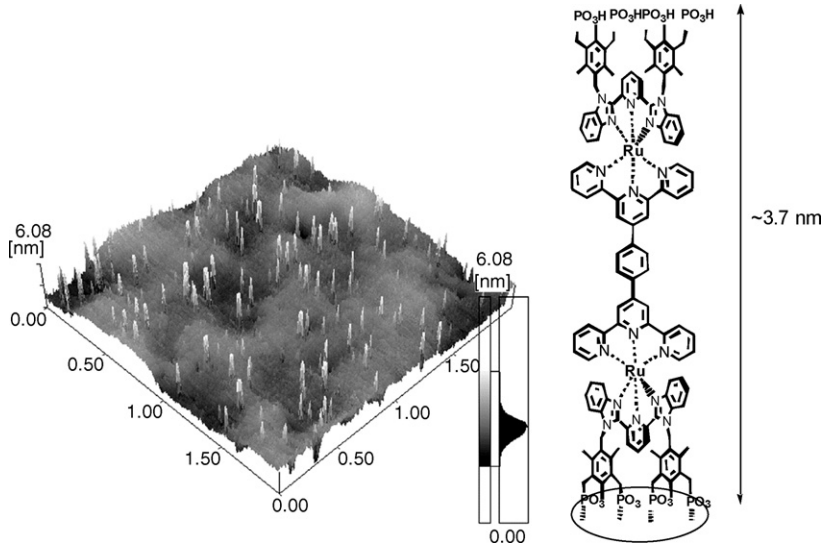

Fig. 1. AFM image of dinuclear $[Ru_2(XP)_2(tpy\text{-}ph\text{-}tpy)]$ complex immobilized on flat ITO substrate and its chemical structure.

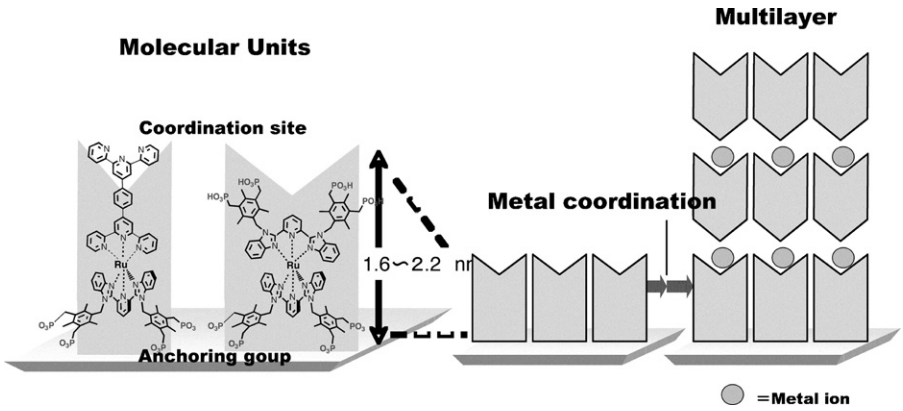

Scheme 7. Layer-by-layer growth by surface coordination chemistry.

al. has demonstrated that a newly synthesized terpyridine thiol ligand allows for the preparation of redox-active mono- and multimetallic systems **3** capable of sequential self-assembly onto gold surfaces [69,70]. These studies show that the anchoring tpy ligand has enough coordination ability to bind other metal ions on the surface [71,72]; however, the importance of free space for coordination has also been pointed out because in the case of closed packed SAMs, little space is available to complete the octahedral environment around the planar tpy ligand.

Furthermore, using two dihydroxamate ligands and eight coordinating metal ions such as Zr^{4+}, Ce^{4+}, and Ti^{4+}, a new kind of multilayer **5** based on metal–ion coordination has been successively built up in a highly controlled step-by-step manner [36,73]. This methodology is applicable for various combinations of C_2-symmetric ditopic ligands and metal ions, resulting in rod-shaped nanoarchitecture with perpendicular orientation to the normal surface.

Not only an organic ditopic ligand but also the metal complex itself can also act as a building molecular linker for multilayer

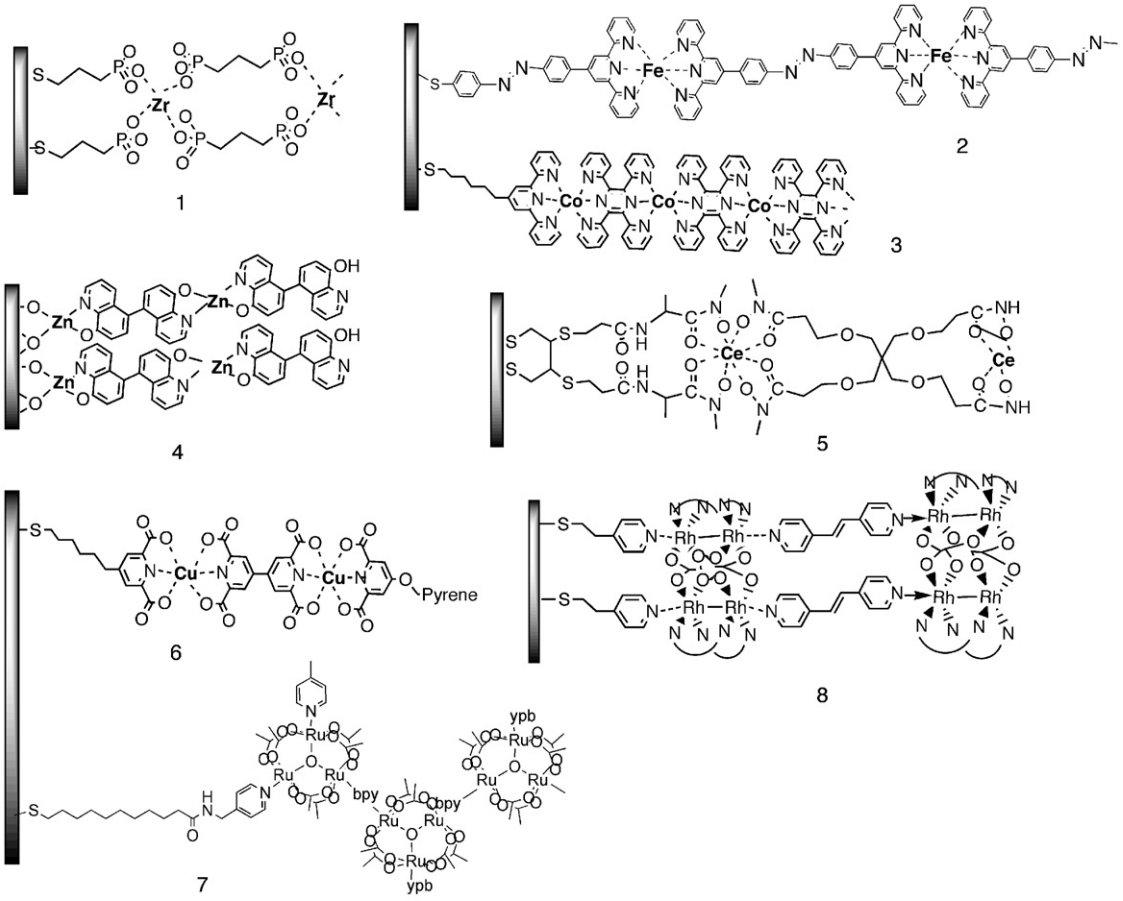

Scheme 8. Examples of LbL structures based on metal complex components fabricated by surface metal coordination. (Structure **1**, Ref. [76]; **2**, Ref. [15a]; **3**, Ref. [70]; **4**, Ref. [15b]; **5**, Ref. [36]; **6**, Ref. [84]; **7**, Ref. [13]; **8**, Ref. [14].)

formation [11,74]. Redox-active Ru/Os complexes with novel tridentate ligands containing two anchoring groups such as phosphonate in Scheme 5 have been synthesized (Scheme 5) [57,75]. These ligands have ideally C_{2v} symmetry, and a bis-tridentate coordination environment at the metal center forces the anchoring groups to point in the opposite direction. Therefore, the LbL growth method was applied for Ru/Os complexes with phosphonate groups. As expected, multilayers with redox-active $M(L)_2$ and $M_2(L)_2$(btpyb) (M = Ru(II) or Os(II), L = LP or XP) units were constructed by the combination of Zr^{4+} or Cu^{2+} ion as a binder. Multilayer formation between phosphonate and metal ions such as Zr^{4+}, Hf^{4+}, or Zn^{2+} was originally developed by Mallouk and co-workers [76,77] on a variety of surfaces via sequential adsorption of metal ions and bis(phosphonic acids) from aqueous solution [78].

One of the advantages of layer-by-layer growth is that a combinatorial approach is feasible using molecular modular units. Since Ru and Os complexes are known to tune their oxidation potentials by the change of ligands and central metal ion, the different ordering of Ru/Os layers from the surface will lead to different potential distribution or gradient in a controlled manner at nanometer size. By changing the order of molecular units with different redox potentials on the surface, any potential sequences toward a molecular rectifier or electron transfer cascade system can be constructed, as described later.

Multilayer formation on the ITO substrate was monitored by various physical measurements such as UV spectra, quartz-crystal microbalance (QCM) and atomic force microscope (AFM). For multilayering experiments of mono- and dinuclear complexes with XP anchor ligand, plots of absorbance for the MLCT band around 500 nm versus the number of layers reveals the linear relationship in all cases. The linearity of the plot of the absorbance versus the number of layers indicated the uniformity of the multilayer structure. Furthermore, STEM images and the depth profile of XPS data were supported by the multilayer structure; therefore, metal complex-based multilayers can be constructed by the combination of redox-active Ru/Os complexes and Zr^{4+} or Zn^{2+} ion.

2.3. Functions of multilayered films

Inorganic LbL multilayer materials based on metal coordination are attractive materials for application in many different fields such as optics, biotechnology, photo- and electrochemistry; i.e., nonlinear optical materials, electroluminescent devices, enzyme sensors, solar energy storage devices, and molecular rectifiers [7,73,79]. Here, we focus on the electrochemical aspects of multilayer architecture on the electrode surface, particularly the rectification effect on the potential gradient system, photocurrent generation, and electrochromic devices.

2.3.1. Potential gradient system

In photosynthesis, photo-induced charge separation is a key process, in which electron transfer takes place through the potential gradient cascade system in order to minimize charge recombination. Extensive studies for mimicking the photosynthetic process have been carried out during the past two decades [80]. The well-ordered multilayer system provides well-defined alignment of the molecular units of sensitizer, electron donors and electron acceptors [54,81]. Within the multilayers, potential gradients assist unidirectional electron transfer to an electroactive substrate, charge separation, and the transport of electrons and holes in opposite directions [82]. The design of molecular rectifiers also requires the arrangement of molecular components in the order of potential gradients.

2.3.2. Photo- and electrochemical devices

SAMs of photoactive chromophores on a gold or ITO surface have been paid much attention as artificial photosynthetic materials and photonic molecular devices. Dye-sensitized photoelectrochemical cells reported by Gratzel et al. employ Ru complexes anchored to the mesoporous nanocrystalline TiO_2 surface together with suitable redox electrolytes or amorphous organic hole conductors [83]. Imahori and Fukuzumi et al. prepared SAMs of porphyrins, porphyrin-fullerene diads or ferrocene–porphyrin–fullerene triads on gold and ITO electrodes, [20,54,55] which lead to photocurrent generation with high efficiency. While conversion efficiency is governed by a product of the efficiency for each process such as light harvesting, photoinduced charge separation, and charge injection, organization of the redox components on solid substrate or electrode has resulted in high quantum yields and longer lifetimes of photoinduced charge-separated states relative to those in solution. Fabrication of photoactive multilayers has been reported, in which Zr^{4+} bisphosphonate multilayers of viologen derivatives on top of copper dithiolate multilayers of porphyrin derivatives on gold electrodes produced efficient and stable cathodic photocurrents by visible light irradiation [81]. Within the multilayer structure, porphyrins as electron donor layers and viologen as electron acceptor layers have been organized in potential gradient arrangement by binders of Zr phosphonate and copper dithiolate (Scheme 9).

As another example, novel multilayer films containing Cu(II), 4,4′-bipyridyl-2,2′,6,6′-tetracarboxylic acid, and capping with the pyrene-containing ligand generated a cathodic photocurrent under photoirradiation [84].

Recently, we prepared a variety of multilayer structures by the combination of redox-active $[Ru(XP)_2]$ and $[M_2(XP)_2$(tpy-ph-tpy)] units (M = Ru or Os), which possess M(II)/M(III) oxidation potentials at +0.65 V, +0.93 V (M = Ru), and +0.64 V (M = Os) versus Ag/AgCl, respectively. In addition, $[Ru(XP)(H_2bip)]$ (H_2bip = bis(benzimidazolyl)pyridine) shows proton-coupled electron transfer reactions, which act as a potential tunable unit on the outmost layer. Therefore, the judicious selection of redox potentials leads to the proper alignment of molecular units with potential gradient in multilayers, which control the direction of unidirectional electron flow.

As a priming first layer, $[Ru(XP)_2]$ and $[M_2(XP)_2$(tpy-ph-tpy)] on an ITO electrode have been immobilized with closed-packed surface coverage of 5.60×10^{-11} and 5.54×10^{-11} mol/cm^2, measured by cyclic voltammogram, respectively. By increasing the number of layers using a Zr(IV) ion linker, the anodic peak current increases linearly up to 14

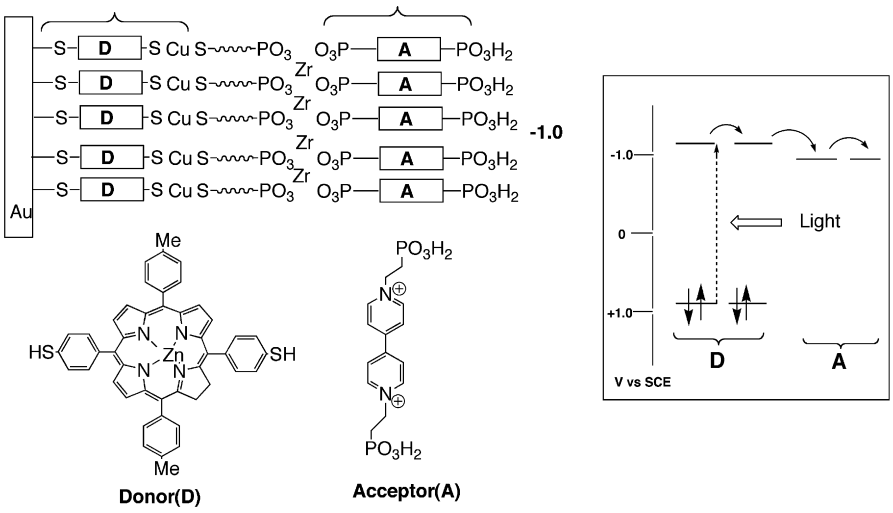

Scheme 9. Photoactive donor–acceptor multilayer systems.

layers for $[Ru(XP)_2]$, and 8 layers for dinuclear $[Ru_2(XP)_2(tpy\text{-}ph\text{-}tpy)]$. Scheme 10 shows three different tri-layered structures, in which the expected potential sequences are also illustrated. In multilayer films, electron transfer occurs preferentially from higher to lower energy through the potential cascade, and therefore from the outer layer to the electrode or vice versa (see Scheme 10).

Cyclic voltammograms of two types of three-layered films on an ITO electrode are shown in Fig. 2, in which the nonequivalence of anodic to cathodic peak ratio was observed; i.e., a larger anodic peak current was mainly observed in the $[Ru(XP)_2]$ complex as a top layer, whereas a larger cathodic peak current was observed in the $[Ru_2(XP)_2(tpy\text{-}ph\text{-}tpy)]$ complex as a top layer, as shown in Fig. 2. This result strongly indicates rectification on multilayer molecular films.

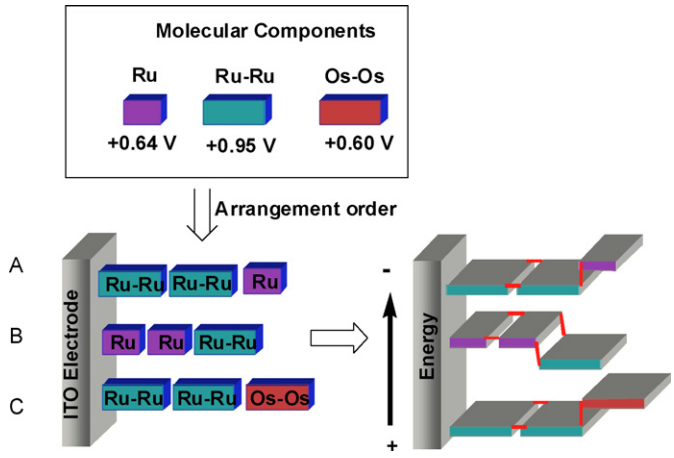

Scheme 10. Three different tri-layered structures with different ordering of molecular units (mononuclear Ru, dinuclear Ru–Ru and Os–Os complexes) and their expected potential sequences.

2.3.3. Electrochromic devices

A wide range of inorganic, organic, and polymeric materials show a visual color change upon oxidation or reduction, which is termed 'electrochromism'. Because of the low absorptivity

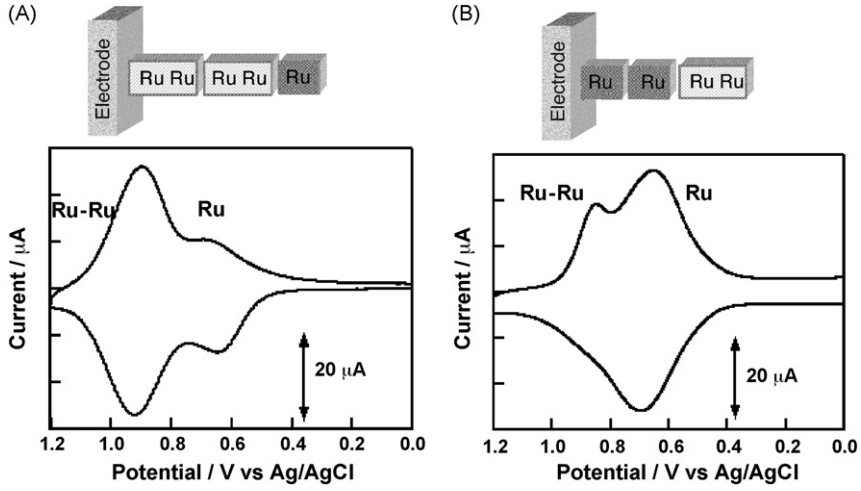

Fig. 2. Cyclic voltammograms of three-layered films for two types (A and B in Scheme 10) on an ITO electrode in 0.1 M $NaBF_4$ (Ref. [59]. ©Springer).

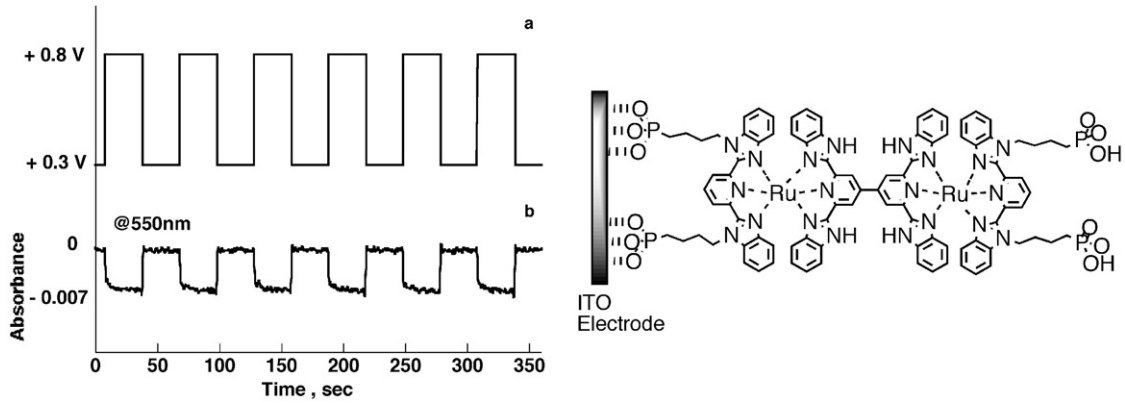

Fig. 3. Electrochromic behavior of Ru dinuclear complex immobilized on ITO electrode: (a) sequence for applied potential and (b) corresponding absorbance change at 550 nm (Ref. [57]. ©The Royal Society of Chemists).

of SAMs, the change of absorbance is quite small to recognize by the naked eye, but a significant gain of absorptivity is attainable by multilayering the units or using polynuclear complexes. Novel dinuclear cyano-bridged mixed valence compounds such as $[Ru^{II}(py)_4(CN)]$-CN-$Ru^{III}(NH_3)_4$pyCOOH immobilized on nanocrystalline SnO_2 or TiO_2 films on conductive glass exhibited electrochromic behavior [85]. Two colored states of these complexes can be interconverted in a narrow potential range (−0.5 to +0.5 V versus SCE) with high stability. The switching times between the two limiting colors is in the order of milliseconds. Similarly, SAMs or multilayers of dinuclear Ru complex on the ITO electrode reveals the electrochromic response at 550 nm in sandwich-type cells [57]. The performance of the cell immobilized by the Ru dinuclear complex on ITO is shown in Fig. 3.

3. Selective anchoring and layering at patterned surface

The patterning, positioning and interconnection of molecules with high accuracy and stability on solid substrates play an important role in molecular electronics [86]. Two different "top–down" and "bottom–up" approaches have been investigated for the fabrication of nanostructures on a solid substrate. For top–down technologies, photolithography-based microfabrication has been developed, which relies on a light wavelength such as visible or UV light. Recently, soft lithography and nanoimprint lithography as a new fabrication method have emerged. On the other hand, bottom–up fabrication uses the self-assembling of molecular units to make a nanostructure. If two metal terminals have a gap of 50 nm on a planar surface, how would one connect these two using molecules? One way is to

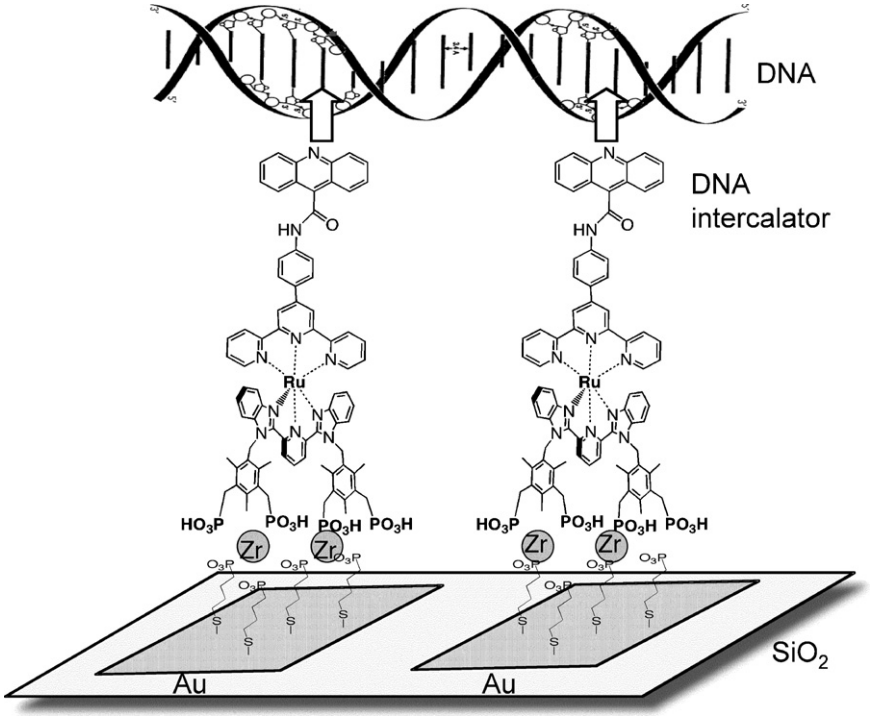

Scheme 11. Schematic illustration of DNA capture between two Ru complexes layered on Zr-MBPA on gold microelectrodes.

synthesize the exact size of the desired molecule, and the other way is to assemble smaller molecular units using SAMs or grafting from molecular units on each terminal by polymerization or the use of a scaffold. As an alternative approach, we have developed a method of DNA wiring between two Au terminals by the assistance of SAM molecules on the surface. DNA template assembly accompanied by a scaffold to a conducting silver wire has been reported for making electronic connections between nanogap electrodes [87]. When DNA trapping molecules are selectively attached to Au terminals of the Au/SiO_2 patterned substrate, DNA molecules can be captured from a solution and used as a scaffold for nanowiring between two Au terminals; therefore, DNA is an attractive material in its usage of a wire scaffold of predetermined length [88]. To date, DNA immobilization can be achieved by electrostatic aggregation [89] or thiol derivatization of DNA for DNA microarrays. Acridine intercalation into DNA has also been used to immobilize DNA on a gold surface. Several methods for DNA expansion, straightening [90], or nanoarchitecture on solid surfaces [91,92] have been reported.

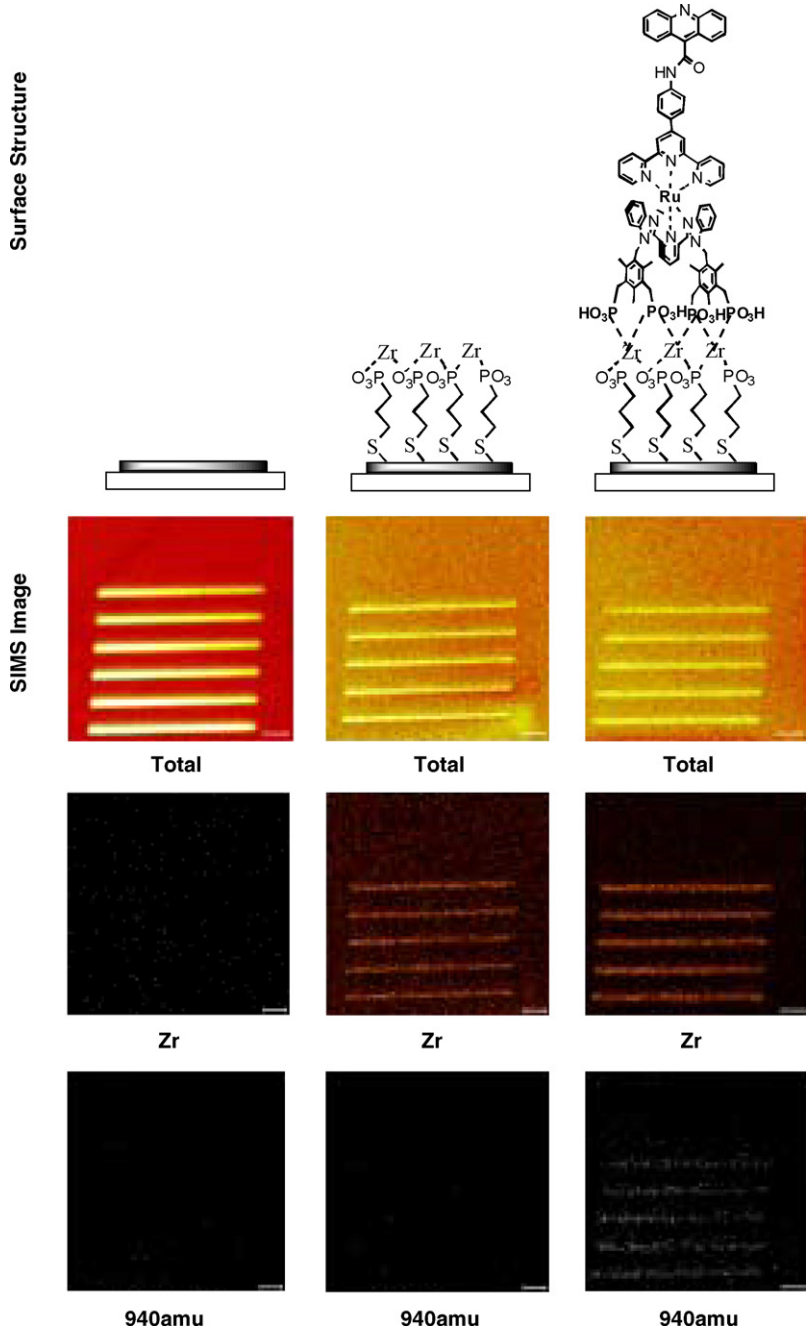

Fig. 4. TOF-SIMS surface images of different stages of surface modification on multilayering (collaboration with Dr. Hisakazu Nozoye at ULVAC-PHI Inc.) (size: 100 μm × 100 μm).

3.1. Selective anchoring and layering on Au/SiO_2 surface

The development of photolithography enables the easy fabrication of micrometer-size Au patterns on a Si wafer. Starting from micrometer-size patterns, the fabrication size can be scaled down by the attachment of "molecular rulers" on the patterns [93]. Further, the importance of the incorporation and interconnection of molecular units into a pre-existing template structure has been pointed out by Allara et al. [86] in order to attach molecular units selectively for the fabrication of molecular-based devices. Along these lines, we have prepared an Au/SiO_2 patterned substrate as a platform for hooking up two Au terminals by a DNA scaffold, and developed a new method of DNA capture by DNA intercalating SAMs immobilized on a Au surface as shown in Scheme 11 [18]. The captured DNAs were used as a scaffold for the metallization or accumulation of chemical substances for chemosensing. As a DNA intercalating group, naphthalene-1,4:5,8-bis(dicarboximide) (ndi) or acridine was selected. Further, several new Ru complexes with anchoring phosphonate groups and a DNA intercalating group have been synthesized and immobilized by orthogonal self-assembly (see Scheme 11).

First, 4-mercaptobutylphosphonic acid was self-assembled on the Au-patterned platform of an Au/SiO_2-patterned silicon wafer, followed by protection of the SiO_2 surface with decylphosphonic acid. Secondly, immersion of the resulting monolayer substrate in $ZrOCl_2$ solution, followed by exposure of the Ru complex/decylphosphonic acid mixtures provides a selectively modified substrate for DNA capture. Selective modification of an Au/SiO_2-patterned substrate has been clearly elucidated by time-of-flight secondary ion mass spectrometry (TOF-SIMS) surface imaging, as shown in Fig. 4. In Fig. 4b, a Zr ion mass peak was clearly seen on the Au-patterned part of the surface, but no peak corresponding to the molecular fragment of Ru complex ($m/z = 940$). On the other hand, after immersion of this substrate in Ru complex solution, the molecular fragment peak of $m/z = 940$ was only observed on the Au-patterned part (see Fig. 4c) in addition to the Zr mass peak part. Selective immobilization of thiol-carboxylate or -phosphonate groups has also been reported by Wrighton et al., but examples of selective layering on a patterned substrate are still limited.

Recently, Reinhoudt and co-workers [94] have reported the "molecular printboard" method, in which molecules can be positioned on printboard using supramolecular microcontact printing and supramolecular dip-pen nanolithography due to specific host–guest interaction between guest "ink" molecules and the modified substrate by host SAMs. A nanoscale pattern can be written and erased on this printboard.

3.2. Molecule-to-molecule connection using ds-DNA toward nanowiring

Several methods have been developed to position and stretch DNA molecules in microelectrode gaps. DNA stretching has been achieved using electrophoresis, [95] optical tweezers, [96] molecular combing by meniscus force, [97] self-organization onto guiding microstructures, [98] and poly(dimethylsiloxane) (PDMS) stamp with DNA "ink" [99]. In our study, the immobilized Ru complex with the DNA intercalating group on a surface interacts with double-stranded DNA (*ds*-DNA) through both intercalation and electrostatic interaction between anionic DNA and cationic Ru complex, and to fix the DNA on a solid surface [100]. Furthermore, molecular combing on the electrode gap facilitates the fixation and stretching of DNA. In the first setup, DNA capture was examined on a mica surface modified by Ru complex. The surface concentration of the Ru complex affects the DNA morphology on the surface; i.e., lower coverage provided a more stretched form of DNA, as described later. Under lower coverage with the Ru complex, the rest of the free space was filled with octylphosphonic acid by self-assembly. AFM images of the surface with low coverage showed scattered dots of almost the same height, consistent with the expected value for the difference between the Ru complex with vertical orientation and octylphosphonic acid by molecular modeling. Using a meniscus transfer method or a pull-up method with a modified mica substrate, λ-DNA was aligned through these immobilized molecular dots in a point-to-point manner (Fig. 5). Both clear lines of DNA and molecular dots of Ru complex were easily discriminated from AFM measurements, as shown in Fig. 5. The molecular height of each DNA line was ∼2.0 nm, and the characteristics were connected in a point-to-point manner associated with sharp break points. Once captured by the immobilized Ru complex, these lines of DNA could not be removed by simple rinsing with water. As a control experiment, DNA was expanded on a bare mica surface by the meniscus transfer method and a clear AFM image of DNA lines was observed; however, these DNA lines were easily washed from the bare mica surface by water, in sharp contrast to the result above.

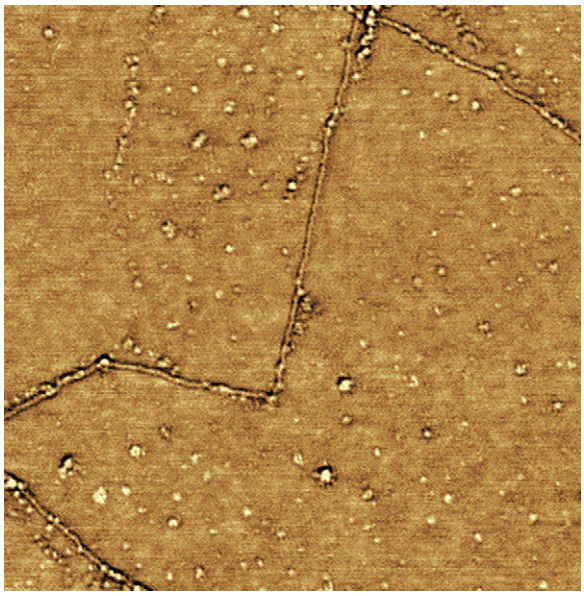

Fig. 5. AFM phase image of DNA captured on mica substrate modified by low coverage of Ru complex. Size: (a) 1.25 μm × 1.25 μm (Ref. [100]. ©Elsevier).

This fixing method of λ-DNAs was applied to a Au/SiO_2 patterned solid surface, resulting in the positioning of DNA in

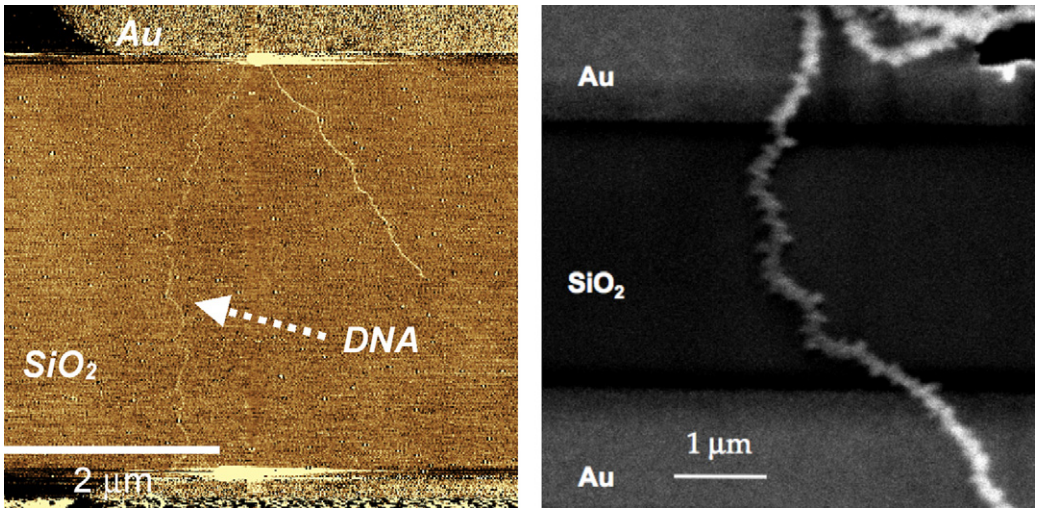

Fig. 6. AFM image of DNA captured between Au terminals modified by Ru complex and octylphosphonic acid (left) and SEM image of DNA nanowire coated with Pd nanoparticles between two Au terminals.

microelectrode gaps (Fig. 6a). The number of captured DNAs depends on the DNA concentration in solution. Fixed DNAs on the substrate surface were covered by cationic Pd nanoparticles, which act as catalysis in electroless copper deposition. Fig. 6b shows SEM images of DNA nanowires covered with Pd nanoparticles and copper metal after electroless deposition, in which the diameter of the nanowire is growing in a step wise manner. Similar wiring by electroless metal deposition has been reported by several groups [98,101]. Fixed DNA nanowires would provide a new reaction environment for preconcentration of chemical materials by interaction or electrostatic attraction, and for a scaffold for nanodevices. He et al. [99] reported the assembly method of highly aligned DNA strands onto Si chips. Using combined molecular combing [97] and microcontact printing (μCP) techniques [102] the orientation of the stretched DNA strands on the surface can be easily controlled. As a result, the aligned DNA strands were bridged across the electrode gaps on the Si chip in stretched form by controlling the contact printing direction perpendicular to the facing microelectrode gaps.

4. Future perspectives for the chemistry of 2D coordination space

Multilayered nanomaterials based on metal complexes can be prepared on a variety of surfaces via sequential metal coordination in a rational way. These nanomaterials have potential applications in a variety of functional systems or devices such as artificial photosynthesis and light harvesting.

Prussian blue, $[Fe^{III}(Fe^{II}(CN)_6)]^-$, is a well-known insoluble mixed-valent complex, in which cubic arrangements of Fe^{n+} centers linked by CN^- bridges build up extended lattices. Prussian blue thin films on an ITO electrode are generally formed by electrochemical reduction of solutions containing Fe(III) and hexacyanoferrate(III) ions [103]. During the redox reaction on the surface, cations are transferred into/from lattices. Using metal–organic frameworks with porosity, the inclusion/exclusion of small molecules or ions will be controlled by an applied potential on the solid surface. Hupp et al. showed that the molecular square based on metal complexes on the electrode recognized the molecular size of chemical materials by current measurements [74,104]. A larger redox-active compound as a marker could not penetrate the void space of the molecular square into the electrode, and therefore no electrochemical response was observed.

Recently, the development of crystal engineering and synthesis of metal–organic frameworks (MOFs) made it possible to design a specific target nanostructure with high porosity [25,105] Several 2D metal–organic coordination networks made by the combination of rigid organic linkers and metal ions on a solid surface such as Cu(1 0 0) or graphite have been synthesized and characterized by STM analysis [106]; however, the 3D MOF system on the surface has not been explored and remains a future challenge since a surface nanostructure with porosity or nanospace will be of great benefit in many practical applications such as gas storage, catalysis, or molecular recognition of chiral catalysis or sensors. In summary, the design of a functional nanostructure on surfaces will play an important role in the development of future material science.

Acknowledgments

M.H. thanks Dr. Hisakazu Nozoye at ULVAC-PHI Inc. for the SIMS imaging measurements. M.H. also acknowledges financial support from the Institute of Science and Engineering at Chuo University and the Ministry of Education, Science, Sports and Culture (Monkasho) for a Grant-in-Aid for Scientific Research (No. 15310076 and 16074215 “Chemistry of Coordination Space”).

References

[1] Y. Wada, M. Tsukada, M. Fujihira, K. Matsushige, T. Ogawa, M.-a. Haga, S. Tanaka, Jpn. J. Appl. Phys. 39 (2000) 3835.
[2] J. Jortner, M. Ratner, Chemistry for the 21st Century Molecular Electronics, Blackwell Science, Oxford, 1997.

[3] C. Joachim, J.K. Gimzewski, A. Aviram, Nature 408 (2000) 541.
[4] M. Fujita, K. Umemoto, M. Yoshizawa, N. Fujita, T. Kurukawa, K. Biradha, Chem. Commun. (2001) 508.
[5] G. Ashkenasy, D. Cahen, R. Cohen, A. Shanzer, A. Vilan, Acc. Chem. Res. 35 (2002) 121.
[6] I. Willner, E. Katz, Angew. Chem. Int. Ed. 39 (2000) 1180.
[7] T.E. Mallouk, H.-N. Kim, P.J. Ollivier, S.W. Keller, Comprehensive Supramolecular Chemistry, vol. 7, Pergamon, 1996, p. 189.
[8] G. Decher, in: G. Decher, J.B. Schlenoff (Eds.), Polyelectrolyte Multilayers an Overview, Multilayer Thin Films, Wiley-VCH, 2003, p. 1.
[9] R.G. Nuzzo, F.A. Fusco, D.L. Allara, J. Am. Chem. Soc. 109 (1987) 2358.
[10] A. Ulman, Chem. Rev. 96 (1996) 1533.
[11] G. Li, W. Fudickar, M. Skupin, A. Klyszcz, C. Draeger, M. Lauer, J.-H. Fuhrhop, Angew. Chem. Int. Ed. 2002 (2002) 1828.
[12] S.D. Evans, A. Ulman, K.E. Goppertberararducci, L.J. Gerenser, J. Am. Chem. Soc. 113 (1991) 5866.
[13] M. Abe, T. Michi, A. Sato, T. Kondo, W. Zhou, S. Ye, K. Uosaki, Y. Sasaki, Angew. Chem. Int. Ed. 42 (2003) 2912.
[14] C. Lin, C.R. Kagan, J. Am. Chem. Soc. 125 (2003) 336.
[15] (a) K. Kanaizuka, M. Murata, Y. Nishimori, I. Mori, K. Nishio, H. Masuda, H. Nishihara, Chem. Lett. 34 (2005) 534;
(b) D.L. Thomsen III, T.P. Bobin, F. Papadimitrkopoulos, J. Am. Chem. Soc. 120 (1998) 6177.
[16] D. Li, D.C. Smith, B.I. Swanson, J.D. Farr, M.T. Paffett, M.E. Hawley, Chem. Mater. 4 (1992) 1047.
[17] C.M. Bell, M.F. Arendt, L. Gomez, R.H. Schmehl, T.E. Mallouk, J. Am. Chem. Soc. 116 (1994) 8374.
[18] M. Haga, Kobunshi 54 (2005) 74.
[19] C.A. Bignozzi, J.R. Schoonover, F. Scandola, Prog. Inorg. Chem 44 (1997) 1.
[20] H. Imahori, M. Arimura, T. Hanada, Y. Nishimura, I. Yamazaki, Y. Sakata, S. Fukuzumi, J. Am. Chem. Soc. 123 (2001) 335.
[21] D. Hirayama, K. Takimiya, Y. Aso, T. Otsubo, T. Hasobe, H. Yamada, H. Imahori, S. Fukuzumi, Y. Sakata, J. Am. Chem. Soc. 124 (2002) 532.
[22] L. Carroll, C.B. Gorman, Angew. Chem. Int. Ed. 41 (2002) 4378.
[23] B. Moulton, M.J. Zaworotko, Chem. Rev. 101 (2001) 1629.
[24] J. Michl, Modular Chemistry, vol. 499, Kluwer Academic Publishers, Dordrecht, 1997.
[25] S. Kitagawa, R. Kitaura, S. Noro, Angew. Chem. Int. Ed. 43 (2004) 2334.
[26] A. Ulman, An Introduction to Ultrathin Organic Films from Langmuir-Blodgett to Self-Assembly, Academic Press, Inc., San Diego, 1991.
[27] I. Kuzmenko, H. Rapaport, K. Kjaer, J. Als-Nielsen, I. Weissbuch, M. Lahav, L. Leiserowitz, Chem. Rev. 101 (2001) 1659.
[28] R.G. Nuzzo, D.L. Allara, J. Am. Chem. Soc. 105 (1983) 4481.
[29] C.D. Bain, E.B. Troughton, Y.-T. Tao, J. Evall, G.M. Whitesides, R.G. Nuzzo, J. Am. Chem. Soc. 111 (1989) 321.
[30] Y. Sato, K. Uosaki, J. Electroanal. Chem. 384 (1995) 57.
[31] H.D. Sikes, J.F. Smalley, S.P. Dudek, A.R. Cook, M.D. Newton, C.E.D. Chidsey, S.W. Feldberg, Science 291 (2001) 1519.
[32] D.A. Offord, S.B. Sachs, M.S. Ennis, T.A. Eberspacher, J.H. Griffin, C.E.D. Chidsey, J.P. Collman, J. Am. Chem. Soc. 120 (1998) 4478.
[33] D. Li, L.W. Moore, B.I. Swanson, Langmuir 10 (1994) 1177.
[34] H.O. Finklea, D.D. Hanshew, J. Am. Chem. Soc. 114 (1992) 3173.
[35] J.J. Hickman, C. Zou, D. Ofer, P.D. Harvey, M.S. Wrighton, P.E. Laibinis, C.D. Bain, G.M. Whitesides, J. Am. Chem. Soc. 111 (1989) 7271.
[36] A. Hatzor, T. Moav, H. Cohen, S. Matlis, J. Libman, A. Vaskevich, A. Shanzer, I. Rubinstein, J. Am. Chem. Soc. 120 (1998) 13469.
[37] G. Cao, H.-G. Hong, T.E. Mallouk, Acc. Chem. Res 25 (1992) 420.
[38] J.J. Hickman, D. Ofer, C. Zou, M.S. Wrighton, P.E. Laibinis, G.M. Whitesides, J. Am. Chem. Soc. 113 (1991) 1128.
[39] M. Haga, H. Hong, Y. Shiozawa, Y. Kawata, H. Monjushiro, T. Fukuo, R. Arakawa, Inorg. Chem. 39 (2000) 4566.
[40] M.-a. Haga, Y. Shiozawa, S. Suzuki, M. Inoue, Mat. Res. Soc. Symp. Proc 679E (2001) B531.
[41] J.T. Woodward, A. Ulman, D.K. Schwartz, Langmuir 12 (1996) 3626.
[42] C. Messerschmidt, D.K. Schwartz, Langmuir 17 (2001) 462.
[43] E.L. Hanson, J. Schwartz, B. Nickel, N. Koch, M.F. Danisman, J. Am. Chem. Soc. 125 (2003) 16074.
[44] H.E. Katz, M.L. Schilling, C.E.D. Chidsey, T.M. Putvinski, R.S. Hutton, Chem. Mater. 3 (1991) 699.
[45] E.S. Gawalt, G. Lu, S.L. Bernasek, J. Schwartz, Langmuir 15 (1999) 8929.
[46] J. Lahann, S. Mitragotri, T.-N. Tran, H. Kaido, J. Sundaram, I.S. Choi, S. Hoffer, G.A. Somorjai, R. Langer, Science 299 (2003) 371.
[47] X. Wang, A.B. Kharitonov, E. Katz, I. Willner, Chem. Commun. (2003) 1542.
[48] B.J. Hong, S.J. Oh, T.O. Youn, S.H. Kwon, J.W. Park, Langmuir 21 (2005) 4257.
[49] E. Galoppini, W. Guo, W. Zhang, P.G. Hoertz, P. Qu, G.J. Meyer, J. Am. Chem. Soc. 124 (2002) 7801.
[50] B. Long, K. Nikitin, D. Fitzmaurice, J. Am. Chem. Soc. 125 (2003) 5152.
[51] K. Nikitin, D. Fitzmaurice, J. Am. Chem. Soc. 127 (2005) 8067.
[52] L. Wei, K. Padmaja, W.J. Youngblood, A.B. Lysenko, J.S. Lindsey, D.F. Bocian, J. Org. Chem. 69 (2004) 1461.
[53] K. Muthukumaran, R.S. Loewe, A. Ambroise, S. Tamaru, Q. Li, G. Mathur, D.F. Bocian, V. Misra, J.S. Lindsey, J. Org. Chem. 69 (2004) 1444.
[54] H. Imahori, H. Norieda, H. Yamada, Y. Nishimura, I. Yamazaki, Y. Sakata, S. Fukuzumi, J. Am. Chem. Soc. 123 (2001) 100.
[55] H. Imahori, H. Yamada, Y. Nishimura, I. Yamazaki, Y. Sakata, J. Phys. Chem. B 104 (2000) 2099.
[56] B. Long, K. Nikitin, D. Fitmaurice, J. Am. Chem. Soc. 125 (2003) 5152.
[57] M. Haga, T. Takasugi, A. Tomie, M. Ishizuya, T. Yamada, M.D. Hossain, M. Inoue, J. Chem. Soc. Dalton Trans. (2003) 2069.
[58] M. Haga, T. Yutaka, in: A.J.L. Pombeiro, C. Amatore (Eds.), Inorganic Supramolecular Architectures at Surfaces, Trends in Molecular Electrochemistry, Marcel Dekker Inc., New York, 2004, p. 311.
[59] M. Haga, in: T. Hirao (Ed.), Nano Redox Sites—Nano-Space Control and Its Applications, Springer, 2006, p. l41.
[60] H. Krass, E.A. Plummer, J.M. Haider, P.R. Barker, N.W. Alcock, Z. Pikramenou, M.J. Hannon, D.G. Kurth, Angew. Chem. Int. Ed. 40 (2001) 3862.
[61] D.M. Guldi, M. Prato, Chem. Commun. (2004) 2517.
[62] H. Zhang, Z. Wang, Y. Zhang, X. Zhang, Langmuir 20 (2004) 9366.
[63] W.B. Stocktont, M.F. Rubner, Macromolecules 30 (1997) 2717.
[64] M.E. van der Boom, P. Zhu, G. Evmenenko, J.E. Malinsky, W. Lin, P. Dutta, T.J. Marks, Langmuir 18 (2002) 3704.
[65] H. Kang, P. Zhu, Y. Yang, A. Facchetti, T.J. Marks, J. Am. Chem. Soc. 126 (2004) 15974.
[66] K. Kim, D. Kim, J.W. Lee, Y.H. Ko, K. Kim, Chem. Commun. (2004) 848.
[67] O. Crespo-Biel, B. Dordi, D.N. Reinhoudt, J. Huskens, J. Am. Chem. Soc. 127 (2005) 7594.
[68] V. Balzani, A. Juris, M. Venturi, S. Campagna, S. Serroni, Chem. Rev. 96 (1996) 759.
[69] Y. Liang, R.H. Schmehl, J. Chem. Soc., Chem. Commun. (1995) 1007.
[70] M. Maskus, H.D. Abruna, Langmuir 12 (1996) 4455.
[71] K.J. Brewer, Commnets Inorg. Chem. 21 (1999) 201.
[72] E.C. Constable, A.M.W.C. Thompson, J. Chem. Soc., Dalton Trans. (1992) 3467.
[73] I. Doron-Mor, H. Cohen, S.R. Cohen, R. Popovitz-Biro, A. Shanzer, A. Vaskevich, J. Rubinstein, Langmuir 20 (2004) 10727.
[74] K.E. Splan, J.T. Hupp, Langmuir 20 (2004) 10560.
[75] Y. Hashimoto, M. Inoue, H. Shindo, M. Haga, J. Inst. Sci. Eng. Chuo Univ. 7 (2001) 29.
[76] J.C. Yang, K. Aoki, H.-J. Hong, D.D. Sackett, M.F. Arendt, S.-L. Yau, C.M Bell, T.E. Mallouk, J. Am. Chem. Soc. 115 (1993) 11855.
[77] H.-G. Hong, T.E. Mallouk, Langmuir 7 (1991) 2362.
[78] H.E. Katz, M.L. Schilling, S. Ungashe, T.M. Putvinski, C.E. Chidsey, ACS Symp. Ser. 499 (1992) 24.
[79] D.B. Mitzi, Chem. Mater. 13 (2001) 3283.
[80] M.R. Wasielewski, Chem. Rev. 92 (1992) 435.
[81] F.B. Abdelrazzaq, R.C. Kwong, M.E. Thompson, J. Am. Chem. Soc. 124 (2002) 4796.

[82] T. Franzl, T.A. Klar, S. Schietinger, A.L. Rogach, J. Feldmann, Nano Lett. 4 (2004) 1599.
[83] A. Hagfeldt, M. Gratzel, Acc. Chem. Res. 33 (2000) 269.
[84] E. Soto, J.C. MacDonald, C.G.F. Cooper, W.G. McGimpsey, J. Am. Chem. Soc. 125 (2003) 2838.
[85] M. Biancardo, P.F.H. Schwab, R. Argazzi, C.A. Bignozzi, Inorg. Chem. 42 (2003) 3966.
[86] D.L. Allara, T.D. Dunbar, P.S. Weiss, L.A. Bumn, M.T. Cygan, J.M. Tour, W.A. Reinerth, Y. Yao, M. Kozaki, A.L. Jones II, Ann. New York Acad. Sci (1999) 349.
[87] D. Porath, G. Cuniberti, R.D. Felice, Top. Curr. Chem 237 (2004) 183.
[88] C.M. Niemeyer, Angew. Chem. Int. Ed. 40 (2001) 4128.
[89] X.-H. Xu, A.J. Bard, J. Am. Chem. Soc. 117 (1995) 2627.
[90] H. Nakano, H. Hayashi, T. Yoshino, S. Sigiyama, K. Otobe, T. Ohtani, Nano Lett. 2 (2002) 475.
[91] H. Yan, S.H. Park, G. Finkelstein, J.H. Reif, T.H. LaBean, Science 301 (2003) 1882.
[92] T.H. LaBean, H. Yan, J. Kopatsch, F. Liu, E. Winfree, J.H. Reif, N.C. Seeman, J. Am. Chem. Soc. 122 (2000) 1848.
[93] A. Hatzor, P.S. Weiss, Science 291 (2001) 1019.
[94] O. Crespo-Biel, B.J. Ravoo, J. Huskens, D.N. Reinhoudt, Dalton Trans. (2006) 2737.
[95] M. Ueda, J. Biochem. Biophys. Methods 41 (1999) 153.
[96] R.M. Simmons, J.T. Finer, S. Chu, J.A. Spudich, Biophys. J. 70 (1996) 1813.
[97] A. Bensimon, A. Simon, A. Chiffaudel, V. Croquette, F. Heslot, D. Bensimon, Science 265 (1994) 2096.
[98] E. Braun, Y. Eichen, U. Sivan, G. Ben-Yoseph, Nature 391 (1998) 775.
[99] J. Zhang, Y. Ma, S. Stachura, H. He, Langmuir 21 (2005) 4180.
[100] M. Haga, M. Ohta, H. Machida, M. Chikira, N. Tonegawa, Thin Solid Films 499 (2006) 201.
[101] J. Richter, M. Mertig, W. Pompe, I. Monch, H.K. Schackert, Appl. Phys. Lett. 78 (2001) 536.
[102] H. Nakao, M. Gad, S. Sigiyama, K. Otobe, T. Ohtani, J. Am. Chem. Soc. 125 (2003) 7162.
[103] K. Itaya, I. Uchida, V.D. Neff, Acc. Chem. Res. 19 (1986) 162.
[104] A.M. Massari, R.W. Gurney, C.P. Schwartz, S.T. Nguyen, J.T. Hupp, Langmuir 20 (2004) 4422.
[105] O.M. Yaghi, M. O'Keeffe, N.M. Ockwig, H.K. Chae, M. Eddaoudi, J. Kim, Nature 423 (2003) 705.
[106] A. Dmitriev, H. Spillmann, N. Lin, J.V. Barth, K. Kern, Angew. Chem. Int. Ed. 42 (2000) 2670.